Understanding the disparate impacts of the 2021 Texas winter storm and power outages through mobile phone location data and nighttime light images

Ryan Zhenqi Zhou[1], Yingjie Hu[1*], Lei Zou[2], Heng Cai[3], and Bing Zhou[2]

[1] GeoAI Lab, Department of Geography, University at Buffalo, NY 14261

[2] GEAR Lab, Department of Geography, Texas A&M University, TX 77843

[3] GIScience for Resilience Lab, Department of Geography, Texas A&M University, TX 77843

Abstract:

Winter Storm Uri slammed Texas between February 13-17, 2021 and caused widespread power outages. Understanding the impacts of this catastrophic event on local communities has important meaning. In this study, we examine the impacts of this winter storm and its impact disparities on different population groups over three stages of this disaster: the initial-hit stage, power-outage stage, and recovery stage. The study focuses on Harris County, Texas which was severely affected by the winter storm. We leverage home-dwelling time information from anonymized mobile phone location data to study the constrained mobility of people due to the winter storm as a way to quantify its impacts on local communities. Considering that mobile phone location data may be affected by the power outages, we further integrate nighttime light (NTL) images into our analyses to assess disaster impacts during the power-outage stage, and use home-dwelling time to assess the impacts during the other two stages (i.e., the initial-hit stage and recovery stage). The results reveal disparate impacts of this winter storm on local communities in the three stages of this disaster. We also find impact disparities on population groups with different socioeconomic and demographic backgrounds, especially during the initial-hit stage. These results help us better understand the impacts of this catastrophic event, and could inform future response and mitigation efforts in identifying vulnerable communities, allocating resources, and curtailing negative impacts of similar disasters.

Keywords:

1. Introduction

Between February 13-17, 2021, a severe winter storm, named Uri, slammed Texas with historically low temperatures, heavy snow, sleet, and freezing rain. This storm brought substantial snowfall

and ice accumulation to many parts of the state, and some areas experienced the coldest conditions in over 30 years [1]. Many power plants and grids in Texas were not prepared to handle the extreme cold; meanwhile, there was a significant increase in the demand for electricity as people rushed to heat their homes [2]. The massive strain on the Texas power grid made its administrators decide to implement rolling blackouts which were supposed to last within an hour each time, but the actual power outages experienced by different households ranged from hours to days across the state [3,4]. Nearly 4.5 million homes in total suffered from power loss in this winter storm [5,6], and various other problems were caused, such as burst water pipes and shortages of water, food, and heat [7]. At least 246 people died directly or indirectly due to the storm, and the total damage was estimated to be over $195 billion [8–10], making Winter Storm Uri the costliest natural disaster in Texas history. Understanding how local communities were impacted by this catastrophic event can help inform future response and mitigation efforts in identifying vulnerable communities, allocating resources, and curtailing the negative impacts of similar disasters.

Existing research has used a variety of data and methods to look into the impacts of Winter Storm Uri. Using surveys and interviews, researchers have studied the resilience of water infrastructures [11], household preparedness [12], and social disparities in power and water outages [13,14]. Using nighttime light images, researchers have identified the geographic areas and neighborhoods that suffered from power outages and analyzed related inequity issues [4,15,16]. Using social media data, researchers have developed methods to assess damages caused by the winter storm [17], and have examined disaster communications by authorities and their interactions with the public [18,19]. There also exist studies that looked into other aspects of this winter storm, such as its mental health impacts [20] and infrastructure interdependence [21].

Anonymized mobile phone location data have received increasing attention since the COVID-19 pandemic [22–24], as they provide a new dimension for studying disrupted human mobility during events like health crises and natural disasters [25,26]. This type of data is typically collected from GPS-enabled smartphones through opt-in software applications (apps), such as navigation, weather, and other apps that need to request user locations (e.g., finding nearby restaurants and gas stations) [27,28]. Location data companies, such as SafeGraph and Advan, sourced these location data from many different apps and aggregated them to areal geographic units (e.g., census block groups) to obtain aggregated mobility patterns. While the data are anonymous and do not contain identity information about individual mobile phone users, they reveal important spatial and temporal patterns of human movement behaviors and visitation to various places, often called points-of-interest (POIs) [29–31]. Given the wide adoption of smartphones [32] and the constant and passive data collection, anonymized mobile phone location data have facilitated disaster studies on fairly large population sizes and in relatively fine temporal resolutions (e.g., impacts on individual days of a disaster).

Researchers have already leveraged anonymized mobile phone location data to study the impacts of Winter Storm Uri. Lee et al. [33] used data from the company Mapbox to study changes in a Mapbox-defined human activity index, and used data from another company SafeGraph to

study changes in visitation patterns to two types of POIs, i.e., grocery stores and restaurants, in Harris County, Texas. Chen et al. [34] also used anonymized mobile phone location data from SafeGraph to reveal the changes in visitations to all POIs during the winter storm focusing on the same geographic area of Harris County. While these previous studies have shed valuable insights, they quantified the disrupted human mobility patterns from a business perspective, i.e., how visits to different POIs, such as grocery stores and restaurants, were affected by the winter storm. This study aims to investigate human responses to winter storms from a residential perspective through the increase of home-dwelling time during the winter storm derived from mobile phone location data. Home-dwelling time was used by researchers previously to study stay-at-home behaviors during the COVID-19 pandemic [35,36]; however, it has been rarely used so far in winter storm research to directly investigate the constrained mobility of residents due to heavy snow.

While home-dwelling time provides useful information for examining the disrupted life of people from a residential perspective, the data may contain an increased level of uncertainty during the power outages triggered by the winter storm. It was reported that many households experienced power outages ranging from a few hours to several days across Texas [2,3]. While typical smartphones can last over several hours, they are unlikely to continuously work for several days; as a result, mobile phone location data during the power-outage period may involve a higher level of uncertainty. With this consideration, we make use of nighttime light (NTL) remote sensing images by learning from the literature [37,4,38,16] to assess the impacts of the winter storm during the power outages.

The objective of this study is twofold. First, we propose to integrate home-dwelling time data with NTL image data to assess the impacts of Winter Storm Uri over three stages: the initial-hit stage, power-outage stage, and recovery stage. Details about the delineation of these three stages are introduced in Section 2. Second, we investigate two research questions (RQs): RQ1: *What were the impacts of Winter Storm Uri on different communities in the three stages of this disaster?* RQ2: *Were there significant differences in the impacts of this winter storm on population groups with different socioeconomic and demographic backgrounds?* The remainder of this paper proceeds as follows. Section 2 describes the study area, time period, and datasets used in this study. Section 3 presents our methods for assessing the impacts of the winter storm on different communities and for examining impact disparities among different population groups. Section 4 reports the obtained analysis results, and Section 5 discusses the results and their implications. Finally, Section 6 concludes this work.

2. Study area and data

2.1. Study area and time period

The study area of this work is Harris County, Texas, which contains the city of Houston and was severely affected by Winter Storm Uri [39,40]. Following the literature [4,16,33], we use census tract as the geographic unit of our investigation, which provides a fairly high spatial resolution for

the analysis. Census tracts are used to approximate communities in this study, and we quantify the impacts of the winter storm on different census tracts as a way to assess its impacts on different communities across the study area. Figure 1 shows the boundaries of Harris County and the studied census tracts.
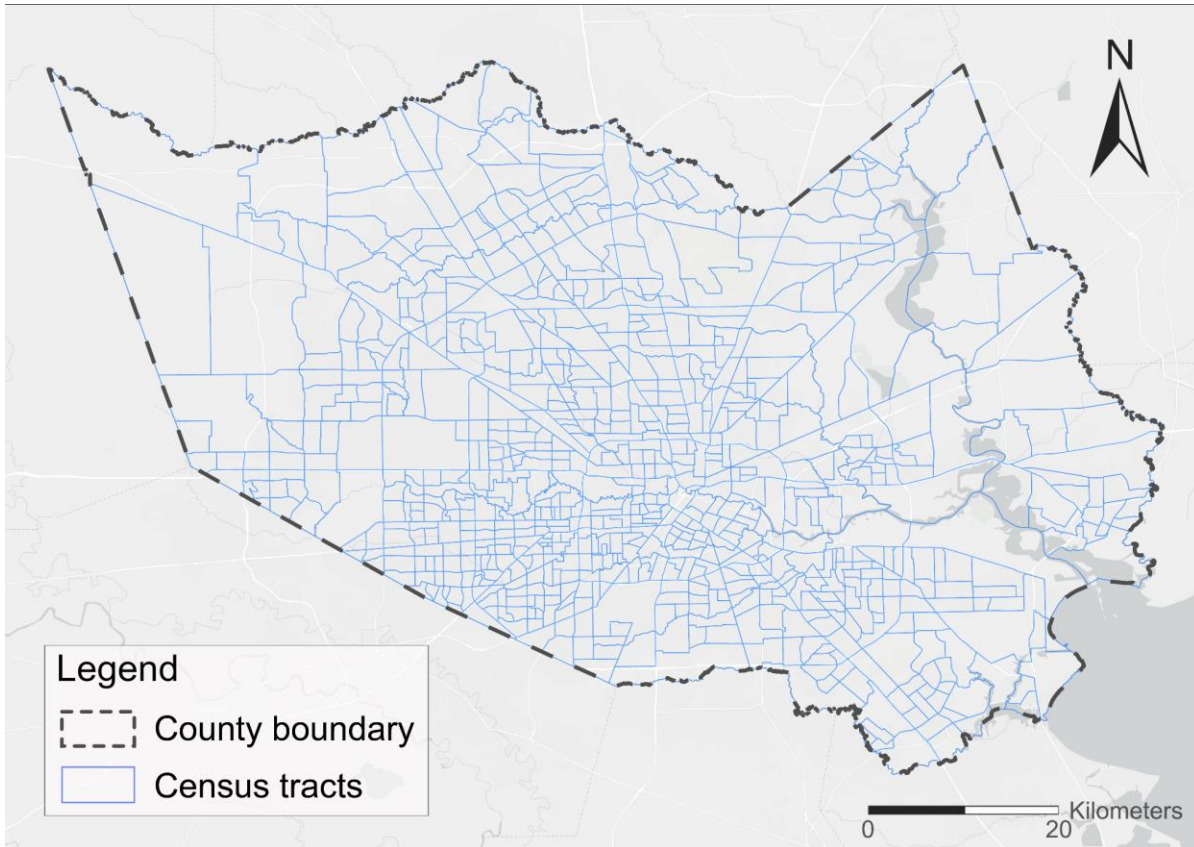

Figure 1. The boundaries of Harris County and the studied census tracts.

For the time period of this study, we examine three stages of this winter storm, which are: initial-hit stage (February 13-14), power-outage stage (February 15-18), and recovery stage (February 19-28). These three stages are determined based on the overall duration of the winter storm in Harris County as documented by NOAA [41] and the county-level power outage data obtained from PowerOutage.us. Figure 2 shows the percentages of households with power outages in Harris County in February 2021. As can be seen, most power outages occurred between February 15-18, and these days are considered as the power-outage stage. The average percentage of power outages in this stage is 17.00%, and the highest percentage is 19.24% on February 16. These high percentages of power outages can be partially attributed to the characteristics of the Texas power system. Texas operates its own power grid separated from the rest of the country. Within this grid, some areas are even more isolated or have fewer connections to other power sources, making them vulnerable to outages when local power generation is disrupted. Meanwhile, areas with older or less robust power transmission and distribution systems were more susceptible to damages from

ice and snow, and infrastructure failures in these areas can lead to prolonged outages during extreme cold conditions.
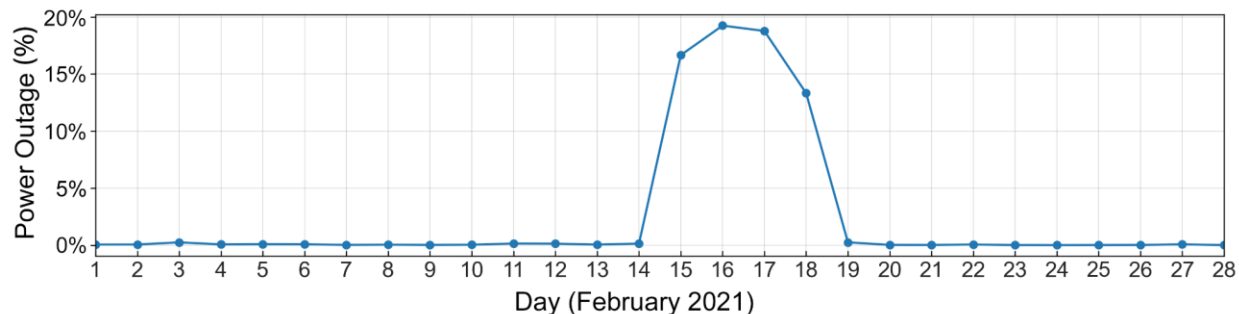

Figure 2. The percentage of households with power outages in Harris County in February 2021 based on data from PowerOutage.us.

2.2. Data

Home-dwelling time from anonymized mobile phone location data. The anonymized mobile phone location data used in this work were obtained from the company SafeGraph which has been widely used in existing research [22,35,33,34]. The whole SafeGraph dataset was collected from about 45 million mobile phones in the US, which cover over 10% of the total US population [42]. In this study, we use such data to study the constrained mobility of people due to the winter storm. SafeGraph creates the home-dwelling time data through two steps: (1) estimating mobile phone users' general home neighborhoods based on their nighttime locations in the past six weeks; (2) calculating the average time that users spend at their homes throughout a day within each block group [43]. The original data were at the census block group (CBG) level. In this study, we aggregate the data to the census tract level using weighted average of the data from the corresponding CBGs within a census tract. More details about data processing are provided in the Methods section.

Nighttime light images. For NTL images, we use VIIRS/NPP Gap-Filled Lunar BRDF-Adjusted NTL images (VNP46A2) from NASA Black Marble as suggested in the literature [37,44,45,4,16]. These NTL images were collected from the Visible Infrared Imaging Radiometer Suite (VIIRS) sensor onboard the Suomi National Polar-Orbiting Partnership (NPP) satellite. They provide high-quality measurements of visible and near-infrared light from the ground with a temporal resolution of daily and a spatial resolution of 500 meters [46]. We aggregate NTL image data to census tracts using a weighted average approach.

Socioeconomic and demographic data. We use the socioeconomic and demographic data from the American Community Survey (ACS) from the US Census Bureau to study the potentially disparate impacts of the winter storm on different population groups. Specifically, we collected four socioeconomic and demographic variables previously identified as robust indicators of disaster resilience in the literature: (1) median household income [25,33], (2) percentage of majority group (non-Hispanic and non-Black) [25,33], (3) median house value [47,48], and (4) percentage of

households having vehicles [47,49]. Based on each attribute, we categorize populations into five different groups by percentile, i.e., Q1 (0%-20%), Q2 (20%-40%), Q3 (40%-60%), Q4 (60%-80%), and Q5 (80%-100%). These population groups allow us to examine the potentially disparate impacts of the winter storm based on each of the four attributes. All socioeconomic and demographic data are prepared at the census tract level.

3. Methods

3.1. Overview of the study design

This research aims to answer two research questions: RQ1: *What were the impacts of Winter Storm Uri on different communities in the three stages of this disaster?* RQ2: *Were there significant differences in the impacts of this winter storm on population groups with different socioeconomic and demographic backgrounds?* To answer these two RQs, we design our research as Figure 3 to examine these three stages in a sequence. For each stage, we perform impact assessment followed by a disparity analysis. We use home-dwelling time from anonymized mobile phone location data to assess impacts of the winter storm in the initial-hit stage and the recovery stage, and we use NTL images to assess its impacts in the power-outage stage. For disparity analyses, we integrate the obtained impact assessment results with socioeconomic and demographic variables to study the impact differences across various population groups. In the following, we provide more details about the used methods for data processing and analysis.
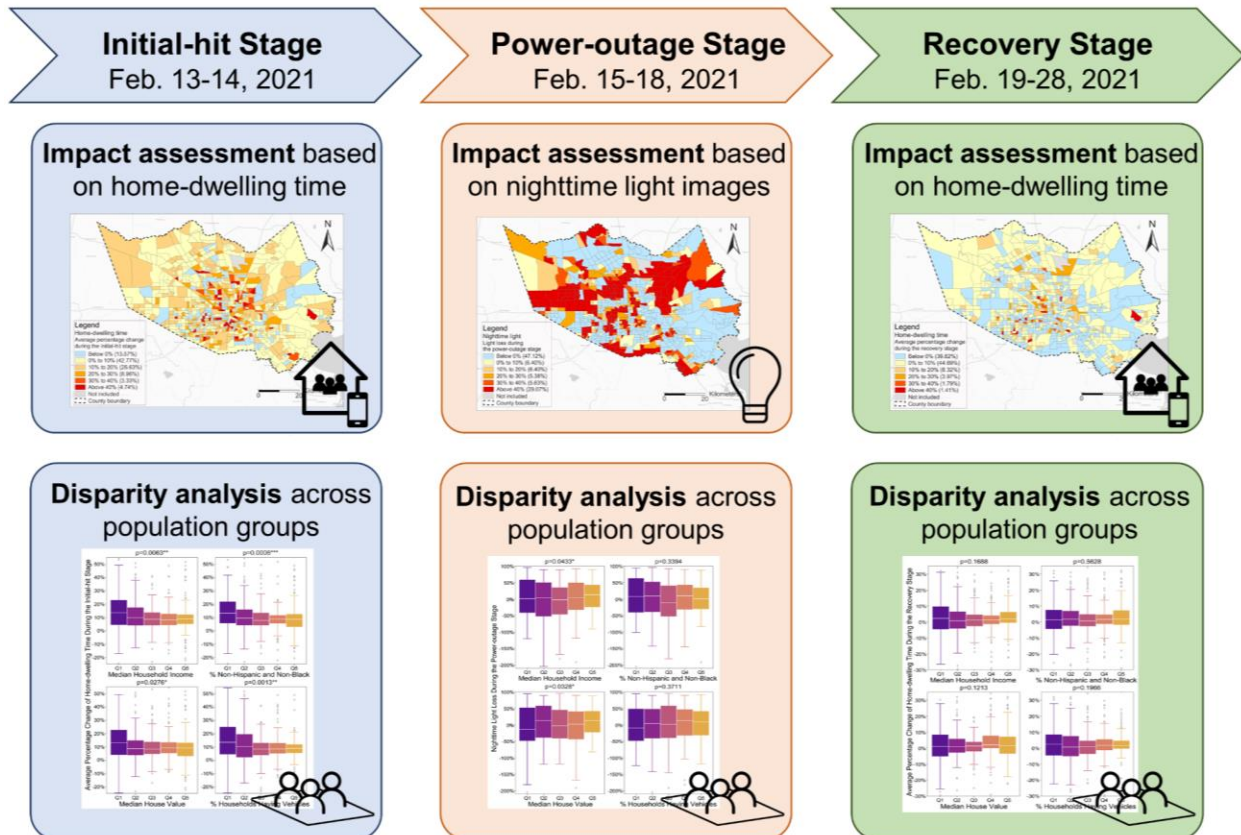
Figure 3. An overview of the study design.

3.2. Impact assessment via home-dwelling time

We assess the impacts of Winter Storm Uri in the initial-hit stage and recovery stage using home-dwelling time from anonymized mobile phone location data. The original data from SafeGraph provide median home-dwelling time of mobile devices residing in a CBG on a daily basis. To obtain census tract level data, we first aggregate the original data from the CBG level to census tract level using a weighted average approach which is summarized in Equation (1):

$$h_j = \frac{\sum_{i=1}^{n} D_i h_i}{\sum_{i=1}^{n} D_i} \qquad , \qquad (1)$$

where h_j is the estimated home-dwelling time for census tract j; n is the number of CBGs within census tract j; D_i is the number of mobile devices residing in CBG_i; h_i is the median home-dwelling time of CBG_i from the original data. To further increase the robustness of our analysis, we remove those census tracts that have fewer than 20 devices to reduce the potential bias that may be introduced by the small numbers of devices in those census tracts. In total, 5 census tracts are removed and 781 census tracts are included in our analysis.

With home-dwelling time estimated for each census tract on each day, we establish home-dwelling time baselines for the analyzed census tracts using their home-dwelling time between January 4 and February 7, 2021 (a total of five weeks). Such a baseline allows a comparison between the stay-at-home time during the winter storm and the normal period without major external disruptions. Considering that the daily home-dwelling time may vary across the week (e.g., people tend to stay home longer on weekends than weekdays), we calculate the median stay-at-home duration for each day of the week for every census tract. Therefore, each census tract has seven baselines of home-dwelling time representing each day of the week.

Next, we quantify changes in home-dwelling time during the initial-hit stage and the recovery stage of the winter storm by comparing the observed home-dwelling time during these two stages with the baselines under normal situations. Equation (2) is used to calculate the changes in home-dwelling time in percentages:

$$c_{jd} = \frac{h_{jd} - b_{jw}}{b_{jw}} \times 100 \qquad , \qquad (2)$$

Where c_{jd} refers to the percentage change of home-dwelling time of census tract j on day d; h_{jd} is the home-dwelling time of census tract j on day d; b_{jw} is the baseline home-dwelling time of census tract j on the weekday w corresponding to day d. For example, if day d is Saturday, February 13, 2021, b_{jw} will be the baseline of census tract j on Saturday. With the percentage changes of home-dwelling time calculated, we then average these change values for each census tract in the initial-hit stage and the recovery stage respectively to quantify the impacts of the winter storm in these two stages.

3.3. Impact assessment via nighttime light images

While changes in home-dwelling time allow us to directly examine the constrained mobility of residents due to the winter storm, mobile phone location data can be affected by the widespread power outages during the winter storm. To address this limitation, we use NTL images to assess the impacts of the winter storm during the power-outage stage. Our analysis largely follows the work by NASA Earth Observatory [50] and the literature [4] which compared the NTL image on February 16 (during the power outage period) with the NTL image on February 7 (during normal time). Meanwhile, we also verify the selection of images on these two dates by examining the Mandatory Quality Flag data from the VNP46N2 NTL images covering the study area. Mandatory Quality Flag data contain important data quality information for each pixel of the NTL images. It has four types of values indicating the quality of pixels: value '00' represents high quality persistent nighttime lights; value '01' represents high quality ephemeral nighttime lights; value '02' represents poor-quality (outlier, potential cloud contamination or other issues); and value '255' represents no retrieval. A closer examination of the quality values of NTL images between February 15 and February 18 reveals that the percentage of high quality pixels (quality values of '00' or '01') in each of these four days are 0.02% (February 15), 99.04% (February 16), 0.00% (February 17), and 0.03% (February 18), respectively. This suggests that only the NTL image on February 16 is satisfactory for examining the impacts, since NTL images on the other days are largely affected by clouds and other issues. Similarly, we check the quality values of NTL images before the winter storm between February 1 and February 12, and find that the image on February 7 has the highest percentage of high quality pixels (99.85%). Thus, we select NTL images on February 7 (for normal time) and February 16 (for power outages) to assess the impacts of the winter storm.

To quantify NTL changes at the census tract level, we first mosaic the images covering the study area on February 7 and February 16 respectively using the software ArcGIS Pro. We then aggregate NTL radiance values from the NTL image pixels to census tracts using weighted average (weighted by the areas of NTL pixels that are counted within each census tract). With NTL values obtained at the census tract level, we calculate the percentage of light loss for each census tract using Equation (3):

$$l_j = \frac{p_j - o_j}{p_j} \times 100 \qquad , \qquad (3)$$

where l_j is the percentage of light loss of census tract j; p_j is the NTL radiance value of census tract j on February 7 (i.e., baseline value during normal time); and o_j is the NTL radiance value of census tract j on February 16 (i.e., power outage time). It is worth noting that the NTL images on these two dates were obtained around 1:00 am Central Standard Time [4,16,50]. Thus, they reflect a snapshot of the power outages at that time, and do not reflect power outages at other times (e.g.,

power outages during the daytime). Nevertheless, NTL images allow us to assess the winter storm's impacts at the time of capture.

3.4. Disparity analysis via Kruskal-Wallis test and Dunn's Test

With impacts assessed for the initial-hit stage, power-outage stage, and recovery stage, we examine the potential disparities in the impacts across different population groups. As described previously, we select four socioeconomic and demographic attributes, and identify five population groups for each attribute based on percentiles. We group the obtained impact metrics to each of the five population groups for each attribute, and use Kruskal-Wallis test and Dunn's test to examine the significance of the difference among the five population groups.

Kruskal–Wallis test is a non-parametric statistical method for testing whether there exists a significant difference among multiple groups. The null hypothesis is that the median values of all groups are equal, and the alternative is that at least one group's median is different from the median of at least another group. In our study, the Kruskal–Wallis test can determine whether there exists at least one group, from Q1 to Q5, that experienced significantly different impacts from the winter storm than at least another group. While the Kruskal–Wallis test detects the presence of such differences, it does not identify the groups that are significantly different. Thus, we further utilize Dunn's test when the result of Kruskal–Wallis test is significant. By applying the Dunn's test to possible group pairs, we can identify the population groups experiencing significantly different impacts and can obtain a fine-grained understanding of the impact disparities based on the four socioeconomic and demographic attributes. We use the *scipy* package in Python to implement Kruskal–Wallis test and *scikit posthocs* package in Python to implement Dunn's test, and the significance level is set as 0.05.

4. Results

4.1. An overview of the home-dwelling time changes and power outages caused by Winter Storm Uri across the three stages

We first provide an overview of the impacts of Winter Storm Uri obtained through our analyses, in Figure 4. The blue lines represent the percentage changes of home-dwelling time of the 781 individual census tracts in the study area, and the red line highlights the average percentage change of all census tracts. As can be seen, most census tracts had increased home-dwelling time during the initial-hit stage of the winter storm, especially on February 14. During the power-outage stage between February 15 and 18, the home-dwelling time change pattern became unclear suggesting the impacts of the power outages on mobile phone location data. In fact, the blue lines of home-dwelling time exhibit a fragmented appearance resembling a "broken rope" during this stage, while the shapes of the rope (i.e., the overall home-dwelling patterns) look much clearer in the other two stages. Thus, we resort to NTL images to assess winter storm impacts during the power-outage stage. During the recovery stage, most census tracts gradually returned to their normal home-dwelling time.
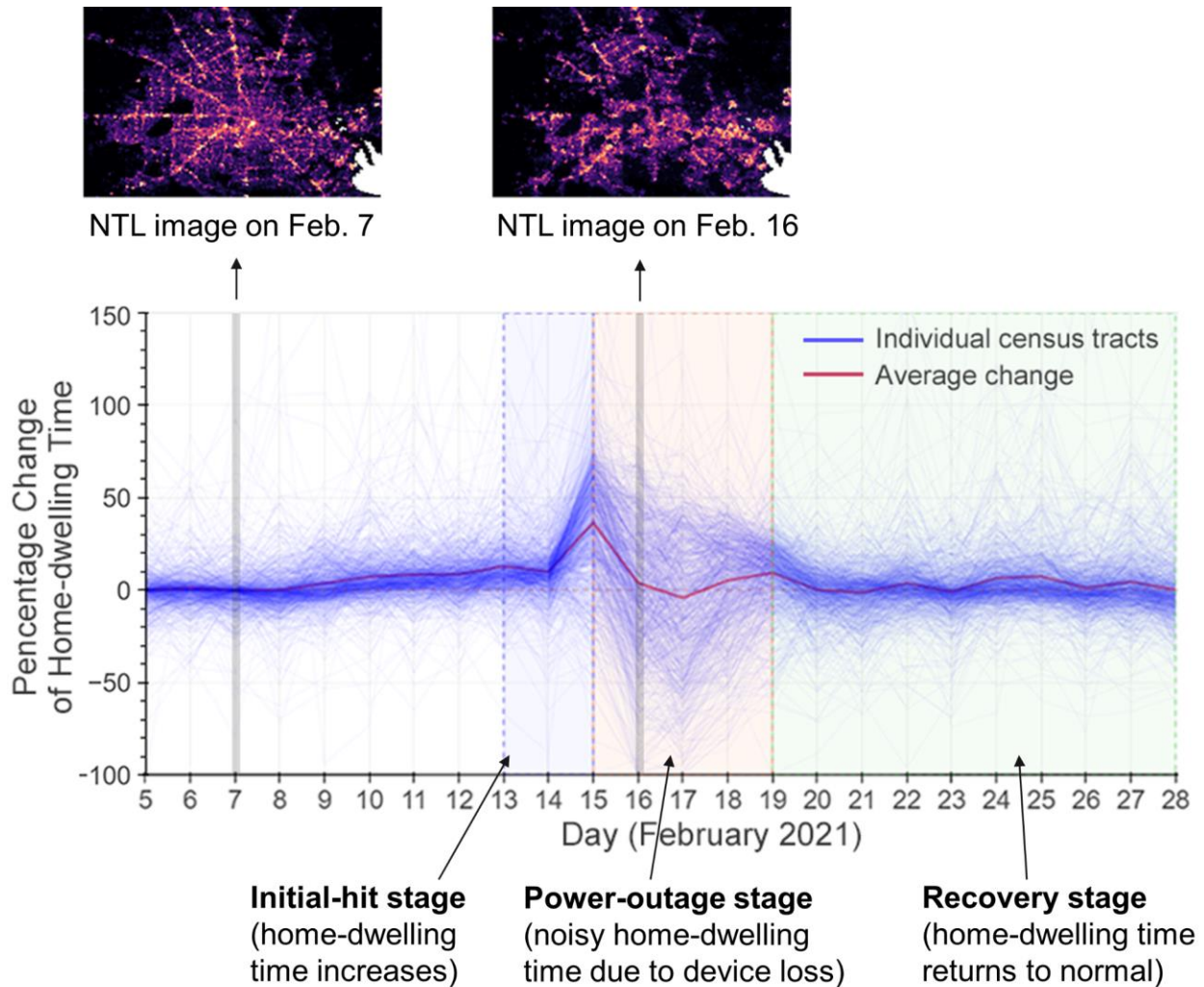
Figure 4. An overview of the impacts of Winter Storm Uri on Harris County over the three stages.

4.2. Impacts and disparities in the initial-hit stage

The impacts of the winter storm in the initial-hit stage are quantified based on home-dwelling time changes, which are visualized in Figure 5. A visual examination of the figure suggests that many census tracts in the central area of the county (i.e., the city of Houston) have larger increases in home-dwelling time compared with census tracts in the peripheral areas of the county. To further quantify the spatial pattern, we leverage the global Moran's I index which measures the overall spatial autocorrelation in the data. The value of global Moran's I ranges between [-1,1], with negative values close to -1 indicating a strong negative spatial autocorrelation (i.e., different values tend to cluster together), and positive values close to 1 indicating a strong positive spatial autocorrelation (i.e., similar values tend to cluster together). Here, the global Moran's I index is 0.033 ($p = 0.083$), suggesting no significant spatial autocorrelation in the home-dwelling time changes. We also perform the local Moran's I analysis to see if any local clusters can be identified, and the result is reported in Supplementary Figure S1. No significant local cluster is identified by

the local Moran's I in this initial-hit stage. The mean and median home-dwelling time changes of all census tracts are 11.34% and 8.98%, respectively, suggesting an overall increase of home-dwelling time during this stage compared with that under normal situations. Nearly half (43.66%) of the examined census tracts have seen a home-dwelling time increase of over 10%, and 8.07% of the census tracts experienced an increase exceeding 30%.
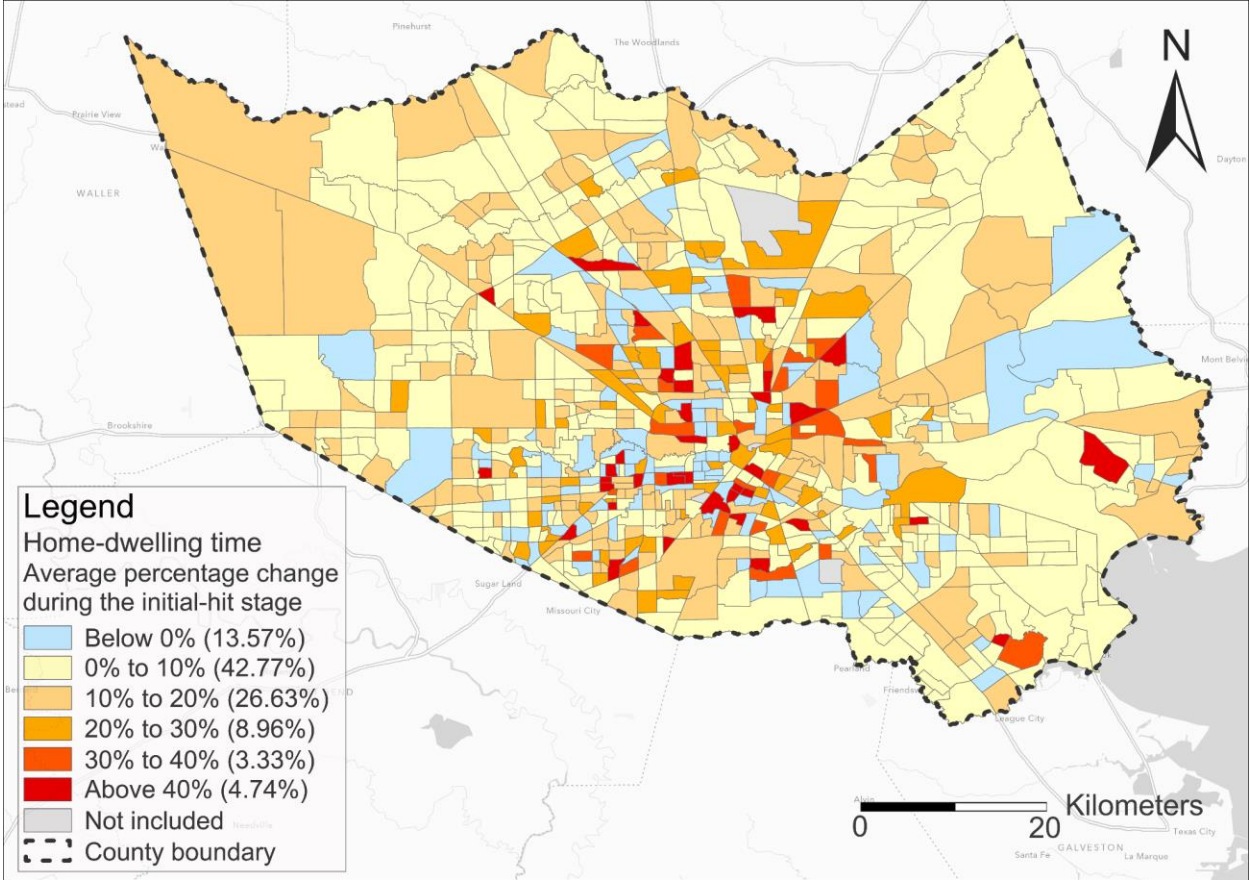

Figure 5. Impacts of the winter storm in the initial-hit stage quantified by the average percentage changes of home-dwelling time of census tracts.

Next, we look into the impacts of the winter storm in the initial-hit stage on different population groups. Figure 6 shows the home-dwelling time changes among the five population groups (Q1 to Q5) characterized by four attributes (data of each attribute are displayed as a subfigure). Different colors in the figure represent different population groups, i.e., Q1 (0%-20%), Q2 (20%-40%), Q3 (40%-60%), Q4 (60%-80%), and Q5 (80%-100%). In addition, p values from the Kruskal-Wallis tests are provided at the top of each subfigure. As can be seen, there exist statistically significant differences among the five groups defined by all four attributes, with p values less than 0.05. We can also visually observe from the figure that those population groups with lower median household income, lower percentage of non-Hispanic and non-Black (i.e., higher percentages of minority population), lower median house value, and fewer vehicles have larger increases in their home-dwelling time and thus higher extents of constrained mobility. The median increases of the

11

Q1 groups across the four attributes are all higher than 10%. By contrast, the median home-dwelling changes of Q2-Q5 groups are lower than 10%, although all groups have increased their home-dwelling time overall.
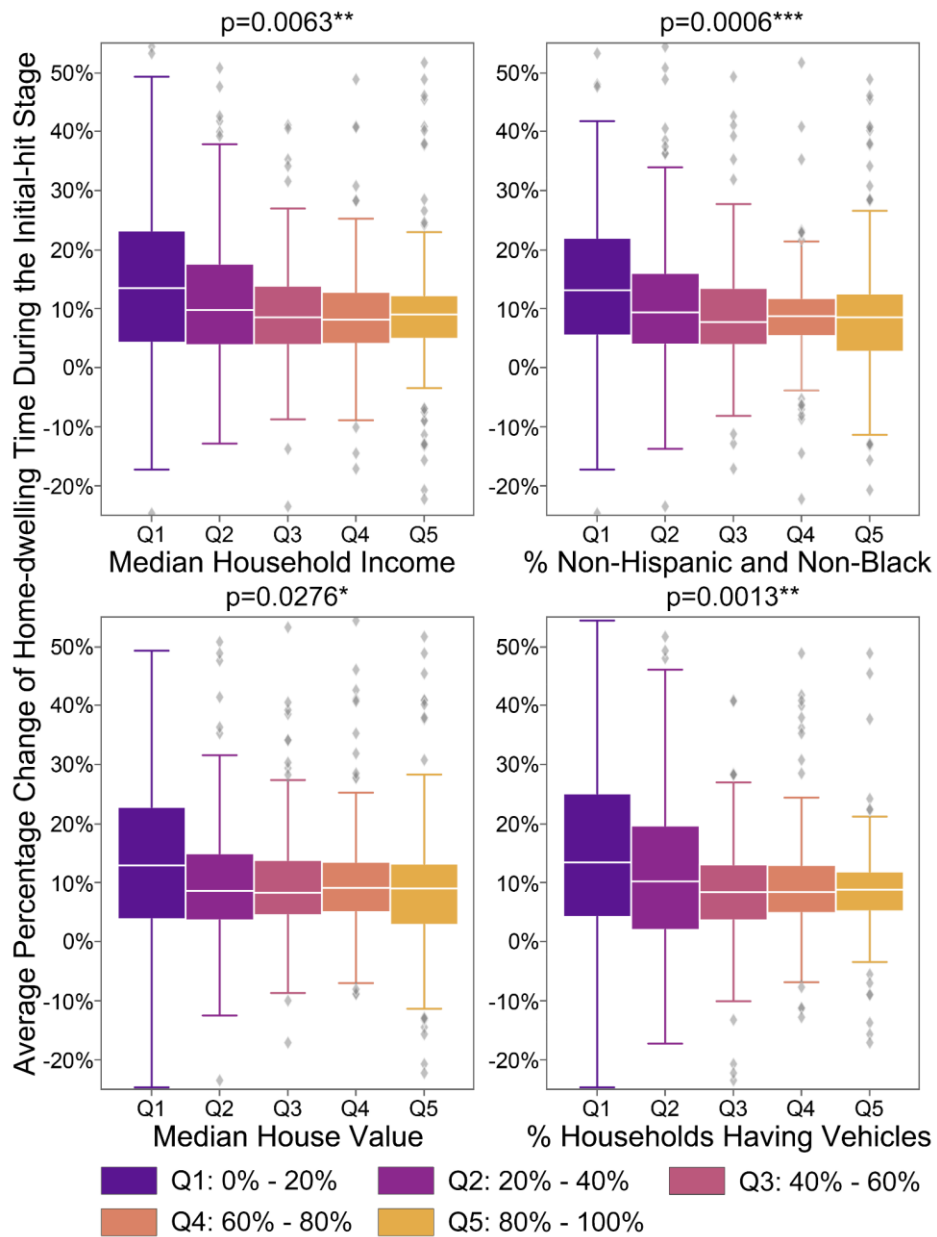

Figure 6. Average percentage changes of home-dwelling time in the initial-hit stage on different population groups (*p-value<0.05; **p-value<0.01; ***p-value<0.001).

Given the significant results of the Kruskal-Wallis tests, we further perform the Dunn's test to identify the specific group pairs whose home-dwelling time changes are different. The results are shown in Figure 7. As can be seen, the home-dwelling time change of Q1 is significantly different from those of Q3, Q4, and Q5 based on *median household income, % non-Hispanic and non-Black,* and *% households having vehicles*. Group Q1 is also significantly different from groups Q2, Q3,

Q5 based on *median house value*. Overall, these results suggest that the winter storm had a higher extent of disruption on the mobility behaviors of the most vulnerable population groups (i.e., the Q1 groups defined by the four attributes) than the other population groups during the initial-hit stage.
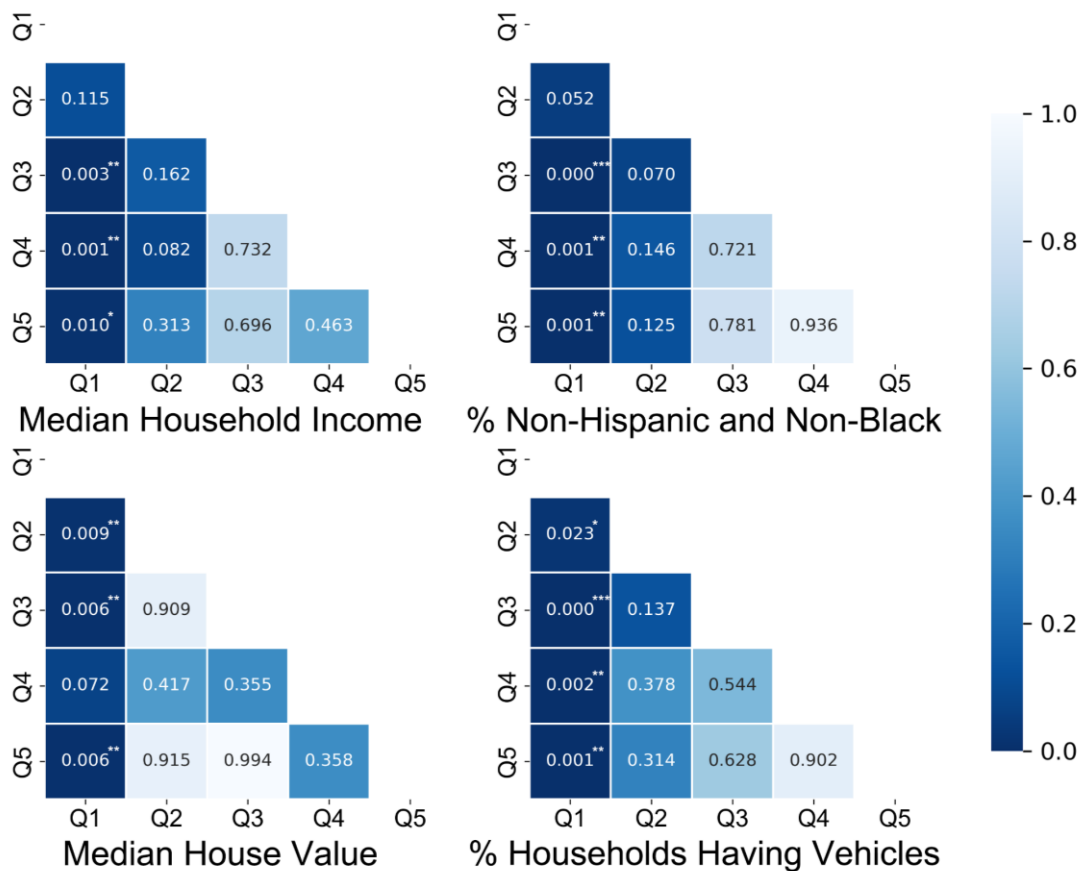

Figure 7. Dunn's test results for population group pairs in the initial-hit stage (*p-value<0.05; **p-value<0.01; ***p-value<0.001).

4.3. Impacts and disparities in the power-outage stage

For the power-outage stage, we use light loss derived from NTL images as an indicator of power outage to assess the impacts of the winter storm. Figure 8 shows the impacts at the census tract level. A visual examination of the figure suggests that the census tracts that have major power loss (above 40%) are clustered in the central, western, northeast, and southern areas of Harris County. By further calculating the global Moran's I index for the light loss, we obtain an index value of 0.585 ($p < 0.001$). This result confirms our visual observation that there exists a significant and positive spatial autocorrelation in light loss, indicating that census tracts that have high light losses tend to cluster together. The result of the local Moran's I analysis, reported in Supplementary Figure S2, also shows multiple major local clusters with high light losses. These results can be attributed to the rotating power outages enforced during the winter storm, as documented by Ferman et al. [3] and Miller [2]. Specifically, census tracts located within the same power outage

13

zones would experience simultaneous power disruptions. The mean and median light losses of all census tracts in this power-outage stage are 2.37% and 3.76%, respectively. While these percentage changes are smaller than the percentage changes in the initial-hit stage (i.e., 11.34% and 8.98%), a direct comparison is not appropriate due to the use of different data types. However, impacts obtained from NTL images in this stage allow us to compare across different census tracts and different population groups.
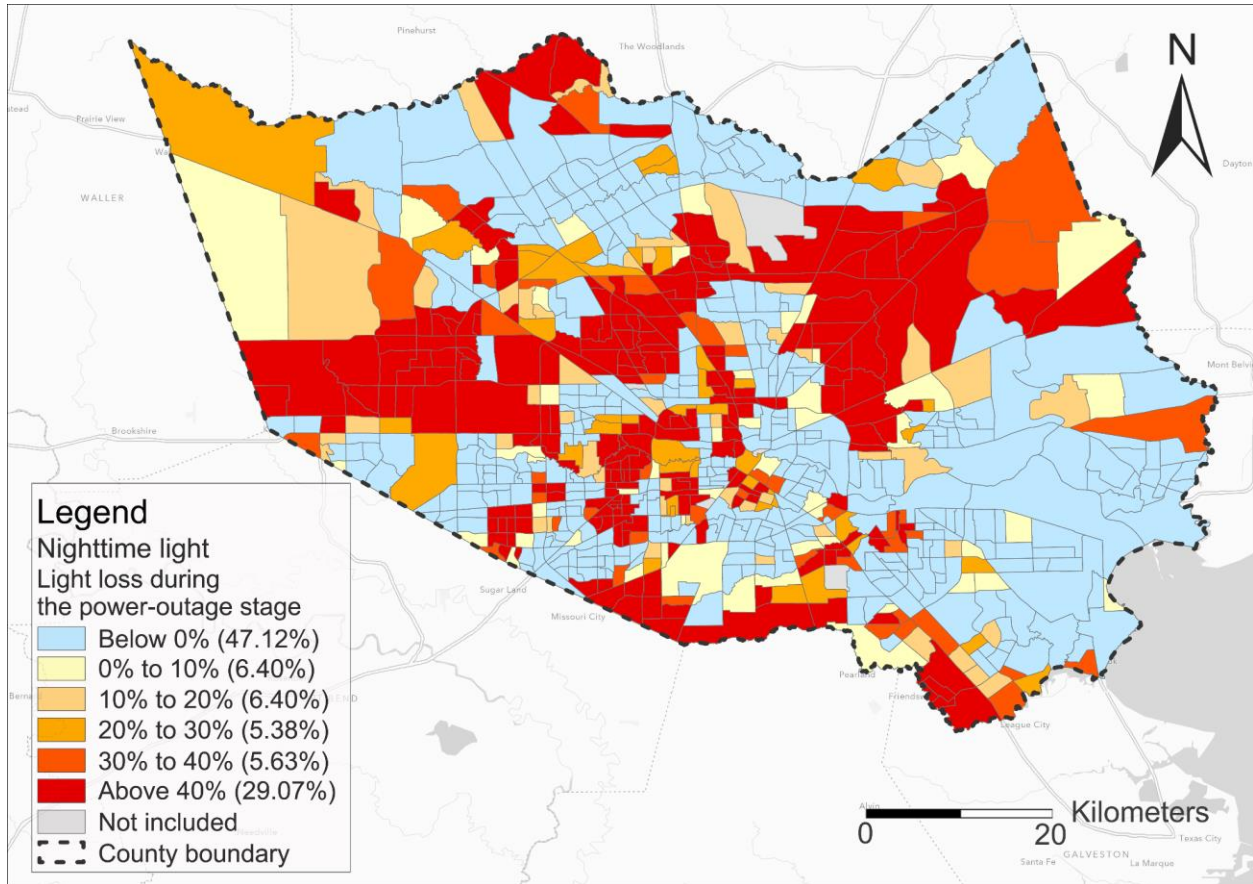

Figure 8. Impacts of the winter storm in the power-outage stage quantified by light loss of census tracts derived from NTL images.

Next, we examine impact disparity across the five population groups defined by the four socioeconomic and demographic attributes. The Kruskal-Wallis tests shown in Figure 9 suggest that there exists significantly different light loss among the groups defined by the attributes *median household income* (upper left) and *median house value* (lower left), with *p* values smaller than 0.05. We can see that the Q5 groups, i.e., census tracts with high median household income and high median house value, experienced comparatively higher light losses (a loss of 12.93% and 12.20% respectively). Kruskal-Wallis tests are insignificant for the population groups based on the other two attributes, suggesting no significant difference in the light loss experienced by the population groups defined by the other two attributes.
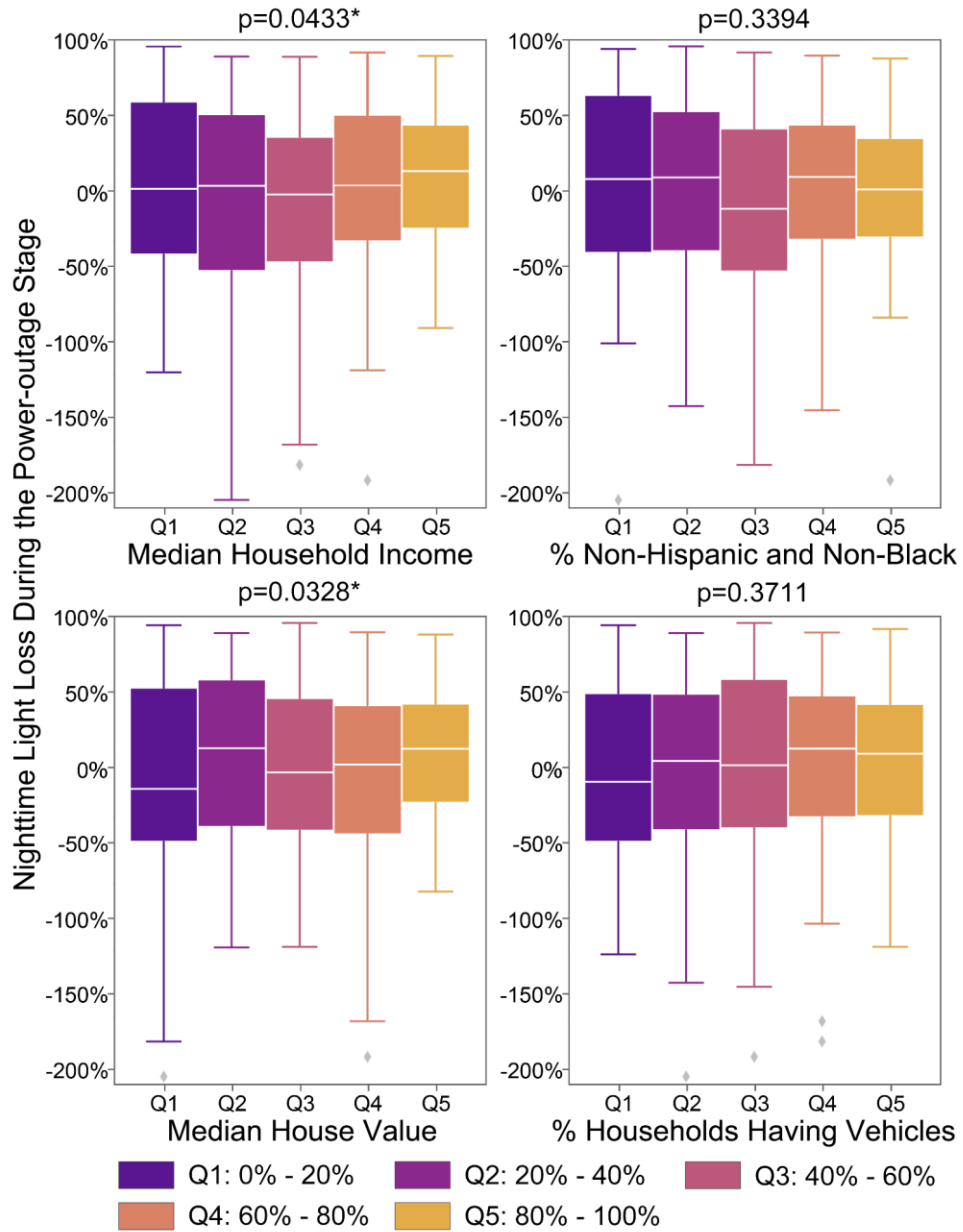
Figure 9. Light loss from NTL images in the power-outage stage on different population groups (*p-value<0.05; **p-value<0.01; ***p-value<0.001).

We further perform the Dunn's test on the population groups defined based on *median household income* and *median house value* (in which Kruskal-Wallis tests are significant) to identify the specific group pairs that have significantly different light losses. The results are shown in Figure 10. As can be seen, group Q5 has significantly different light loss compared with Q2 and Q3 based on *median household income,* and the group Q4 also has significantly different light loss compared with Q3. For the groups defined by *median house value*, groups Q5 and Q2 have significantly different light loss compared with group Q1. Note that the light loss is calculated based on NTL images on February 16th at about 1:00 am compared with images on February 7th

at around the same time; thus, it provides a snapshot of the light changes at that specific time and does not represent the light loss of the entire power-outage stage.
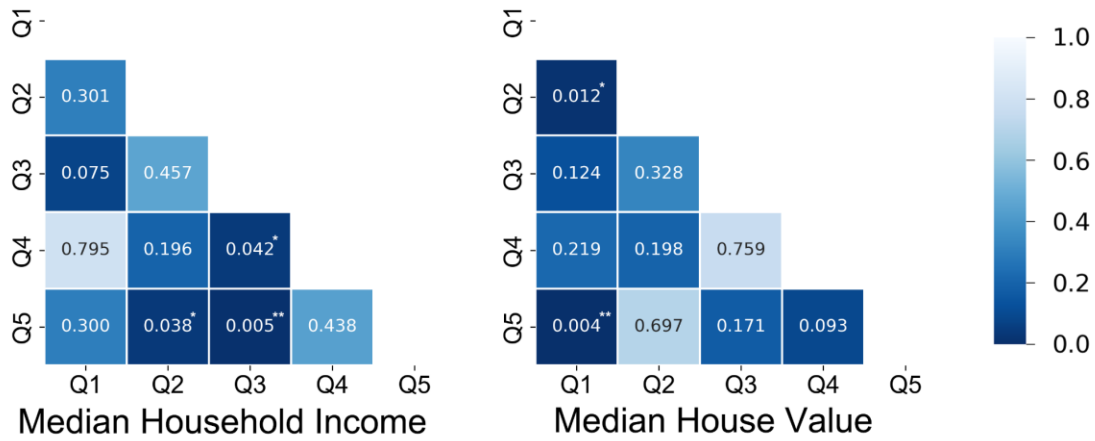

Figure 10. Dunn's test results for population group pairs in the power-outage stage based on *median household income* and *median house value* (*p-value<0.05; **p-value<0.01; ***p-value<0.001).

4.4. Impacts and disparities in the recovery stage

The impacts of the winter storm in the recovery stage are assessed using percentage changes in home-dwelling time, given that power is mostly restored during this stage (as shown in the power-outage data in Figure 2). The obtained impacts are provided in Figure 11. Overall, most of the census tracts (84.51%) only have minor increases in home-dwelling time. The mean and median home-dwelling time changes are 3.04% and 1.52%, respectively. These changes are much smaller than the home-dwelling time changes in the initial-hit stage (i.e., 11.34% and 8.98%), suggesting that the life of people is gradually returning to normal, and the constrained human mobility is being relieved. A visual examination of the map does not identify a clear spatial pattern in the home-dwelling time changes. The global Moran's I index is 0.022 ($p = 0.240$), indicating no significant spatial autocorrelation. No significant local cluster is identified by the local Moran's I analysis in this recovery stage, as shown in Supplementary Figure S3.
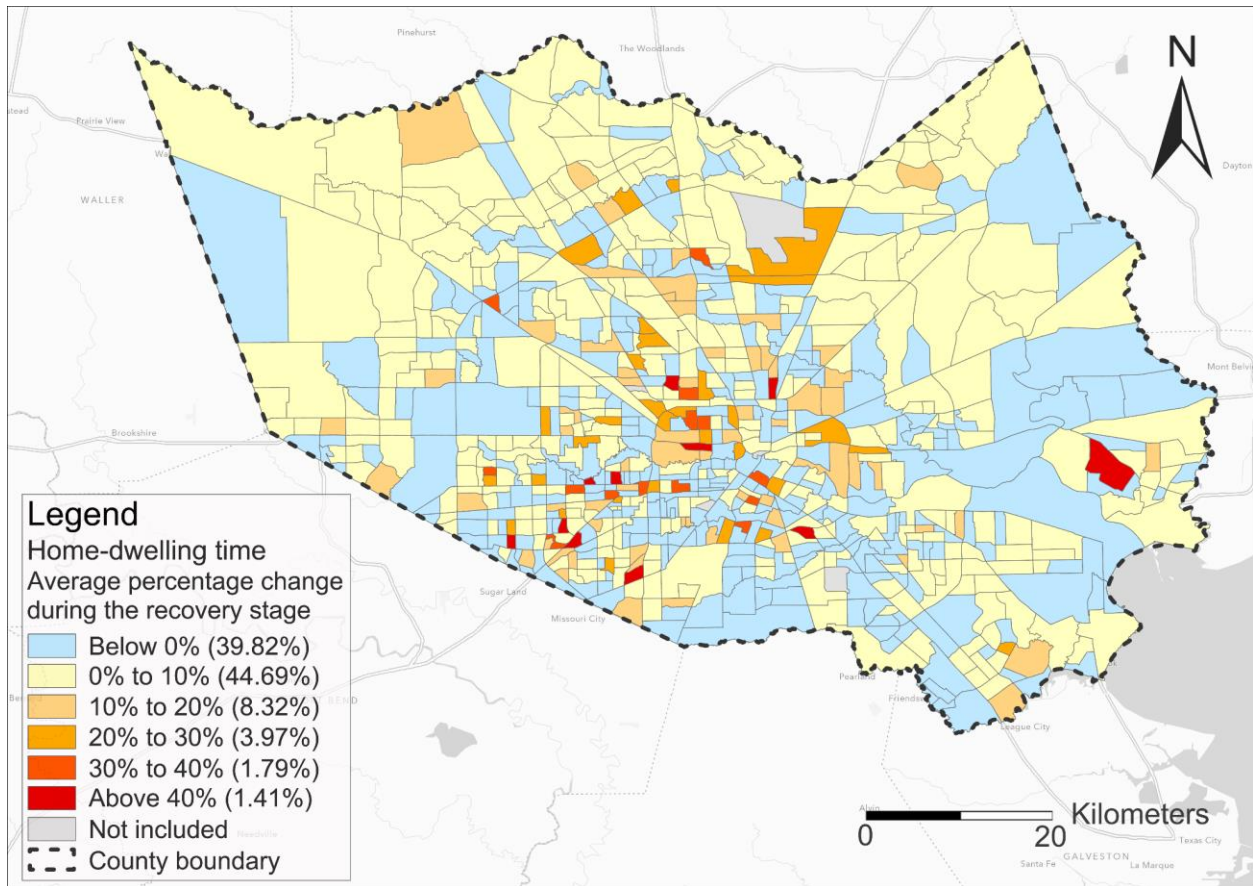
16

Figure 11. Impacts of the winter storm in the recovery stage quantified by the average percentage changes of home-dwelling time of census tracts.

Next, we examine impact disparity across different population groups in this stage. The data visualization and Kruskal-Wallis test results are shown in Figure 12. The results of the Kruskal-Wallis tests suggest no significant discrepancy in the home-dwelling time changes of different population groups based on all four attributes (p values are all larger than 0.05), indicating that no group has a significantly different home-dwelling time change than other groups during the recovery stage. Visual interpretation suggests that there are slight rises in median home-dwelling time for all population groups compared with their normal home-dwelling time. However, the increases are overall similar across different groups. Given the insignificant results from the Kruskal-Wallis tests, we do not further perform Dunn's tests.
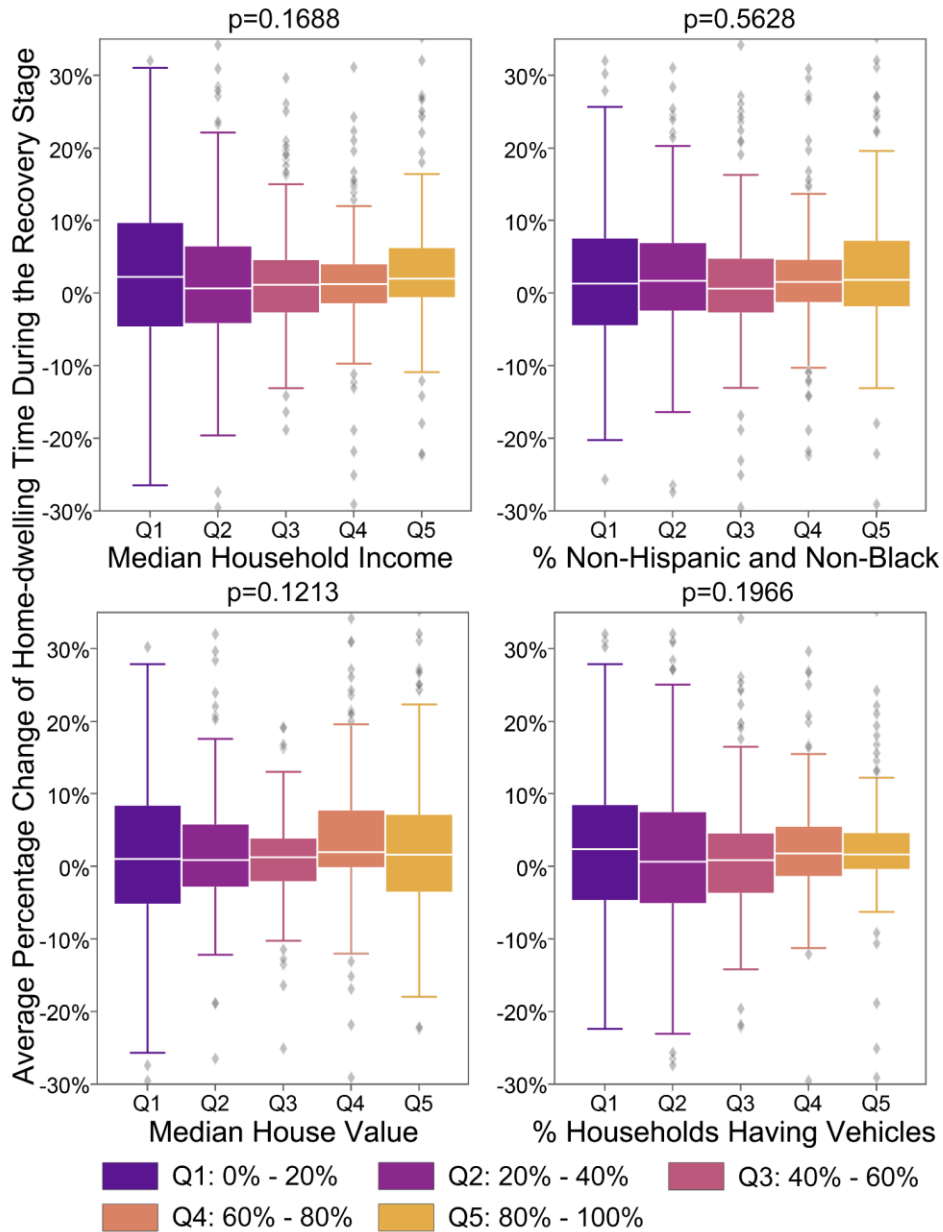
Figure 12. Average percentage changes of home-dwelling time in the recovery stage on different population groups (*p-value<0.05; **p-value<0.01; ***p-value<0.001).

5. Discussion

The results of our analyses have revealed the impacts of Winter Storm Uri, in the forms of changed home-dwelling time and power outages, over three stages and its impact disparities on different population groups. To answer RQ1: *What were the impacts of Winter Storm Uri on different communities in the three stages of this disaster*, our study has found that there was a relatively large increase of home-dwelling time (an average increase of 11.34%) among the studied census tracts in the initial-hit stage; there was an average light loss of 2.37% based on NTL images (the

percentage change based on NTL cannot be directly compared with the percentage change based on home-dwelling time); and there was a relatively small increase of home-dwelling time (an average increase of 3.04%) in the recovery stage. From a spatial perspective, census tracts in the central area of Harris County (i.e., within or close to the City of Houston) had higher increases in home-dwelling time than census tracts in the peripheral areas in the initial-hit stage and the recovery stage; during the power-outage stage, census tracts in both central and peripheral areas suffered from major power loss, demonstrating significant spatial clustering patterns likely related to the rolling blackouts implemented in this winter storm. To answer RQ2: *Were there significant differences in the impacts of this winter storm on population groups with different socioeconomic and demographic backgrounds*, our study has improved our understanding of impact disparities across the three stages based on the analyzed socioeconomic and demographic attributes. In the initial-hit stage, population groups in Q1 (i.e., the most vulnerable population groups) in terms of median household income, percentage of non-Hispanic and non-Black population, median house value, and percentage of households having vehicles suffered from higher extents of constrained mobility than most other population groups. In the power-outage stage, population groups in Q5 in median household income and median house value were affected by higher extents of light loss based on a snapshot of NTL images on February 16th at around 1:00 am. This result suggests that the rotating power outages were likely intended to be fair, although communities with older power grids and less robust power infrastructures could be affected more for the entire power-outage stage. In the recovery stage, no significant disparity was observed across the different population groups based on the four studied socioeconomic and demographic attributes.

Our study complements the existing literature on Winter Storm Uri in two aspects. First, we provide a residential perspective for understanding the impacts of the winter storm. While mobile phone location data have already been used in previous research on Winter Storm Uri [33,34], existing studies generally take a business perspective by examining how visits to different POIs, such as restaurants, grocery stores, and shopping centers, are disrupted by the winter storm. Our work directly assesses the constrained mobility of residents due to the winter storm by examining home-dwelling time changes, and therefore provides a complementary perspective on how the normal mobility of residents was disrupted. Considering that home-dwelling time data can be affected by the power outages, we integrate NTL images into our study and utilize NTL images to fill the gap of the home-dwelling time data. Second, our study reveals the impacts of Winter Storm Uri and its impact disparities over three stages of this disaster. Existing research has either examined the winter storm as one whole time period or focused on only a few important days of the storm [33,4,34]. Our study, therefore, provides results with a finer temporal granularity and helps understand the different impact disparities over the three stages of the winter storm.

This study has potential implications for emergency management policies and future disaster research. The revealed disparate impacts of the winter storm on different population groups could inform emergency management policies by pinpointing the communities severely affected by the storm, identifying vulnerable population groups, and improving the allocation of emergency resources. This study, along with other existing research on Winter Storm Uri [4,33,34], also

further highlights the limitations of the current Texas power grid under extreme cold conditions, and could inform future efforts and policies on improving power generation, power distribution, and other aspects of the power infrastructures. For future disaster research, this study provides a methodological framework on integrating mobile phone location data and nighttime light images, which can be used in future research to investigate the multifaceted impacts triggered by a disaster. As one of the early studies taking a residential perspective to examine human responses to winter storms, this work also generates baseline information that can be compared with in future studies regarding the impacts of disasters on the mobility of residents and the subsequent recovery process.

Several limitations are worth noting. First, the impact assessment during the power-outage stage is based on the NTL images on February 16 at about 1:00 am, and does not reflect the electricity disruption of the entire power-outage stage. NTL images on the other days of the power-outage stage cannot be used unfortunately, due to insufficient data quality caused by clouds and other noise issues. While our analysis based on NTL images on February 16 does provide a snapshot of the impacts of the winter storm, a more comprehensive assessment could be conducted when more detailed power-outage data become available. We note that the power outage data obtained from PowerOutage.us is at the county level and are not detailed enough for examining power outages of spatial units smaller than counties (e.g., census tracts in this study). Second, while we use mobile phone location data only during the initial-hit and recovery stages when power was available for most households, it is possible that some mobile phones might not recover quickly after the power outages. These mobile phones could have some effects on the analysis results in the recovery stage and could be further investigated. Third, our impact disparity analyses are based on four socioeconomic and demographic attributes only, i.e., *median household income*, *percentage of non-Hispanic and non-Black population*, *median house value*, and *percentage of households having vehicles*. These four attributes have been widely adopted in previous research to study vulnerable populations under the context of natural disasters [47,49,25,33]. Nevertheless, other attributes, such as percentage of elderly population and percentage of households with children, could also be investigated to further understand the impact disparities across different population groups. The same methodological framework and statistical tests used in this research could also be utilized to study these other socioeconomic and demographic attributes in future.

6. Conclusions

The 2021 Texas winter storm, or Winter Storm Uri, was a catastrophic event that severely impacted the lives of millions of people. This study examines the impacts of this winter storm and its impact disparities in three stages of this disaster: the initial-hit stage, power-outage stage, and recovery stage. We leverage home-dwelling time information from anonymized mobile phone location data to study the constrained mobility of people due to the winter storm in the initial-hit stage and the recovery stage. Considering that mobile phone location data may be affected by power outages, we further integrate NTL images into our analyses to assess the impacts during the power-outage stage. We investigate the impact disparities of this winter storm on different population groups by

four socioeconomic and demographic attributes using statistical tests. Our analysis results provide detailed information about the impacts of this winter storm on different census tracts in Harris County over the three stages. We also find disparate impacts of this winter storm on different population groups, especially on vulnerable population groups during the initial-hit stage. Overall, this work offers a residential perspective at a fine temporal granularity for improved understanding of the disparate impacts caused by Winter Storm Uri on local communities.

Abbreviations

NTL: Nighttime Light

POI: Point of Interest

CBG: Census Block Group

VIIRS: Visible Infrared Imaging Radiometer Suite

NPP: National Polar-Orbiting Partnership

ACS: American Community Survey

Declaration of competing interest

The authors declare that they have no competing financial interests or personal relationships that could have appeared to influence the work reported in this paper.

Data availability

Data will be made available on request.

Acknowledgements

References

[1] C. Maxouris, Here's how a week of frigid weather and catastrophe unfolded in Texas, CNN (2021). https://www.cnn.com/2021/02/21/weather/texas-winter-storm-timeline/index.html.

[2] R.M. Miller, Massive failure': Why are millions of people in Texas still without power, Tysons VA USA Today (2021).

[3]   M. Ferman, S. Sparber, E. Limón, 2 million Texas households without power as massive winter storm drives demand for electricity, Tex. Trib. (2021).

[4]   A. Nejat, L. Solitare, E. Pettitt, H. Mohsenian-Rad, Equitable community resilience: The case of Winter Storm Uri in Texas, Int. J. Disaster Risk Reduct. 77 (2022) 103070. https://doi.org/10.1016/j.ijdrr.2022.103070.

[5]   W. Englund, The Texas grid got crushed because its operators didn't see the need to prepare for cold weather, Wash. Post (2021). https://www.washingtonpost.com/business/2021/02/16/ercot-texas-electric-grid-failure/ (accessed March 21, 2022).

[6]   B. Sullivan, N. Malik, 5 Million Americans Have Lost Power After a Devastating Winter Storm, Time (2021). https://time.com/5939633/texas-power-outage-blackouts/ (accessed March 21, 2022).

[7]   O.E. Adepoju, D. Han, M. Chae, K.L. Smith, L. Gilbert, S. Choudhury, L. Woodard, Health Disparities and Climate Change: The Intersection of Three Disaster Events on Vulnerable Communities in Houston, Texas, Int. J. Environ. Res. Public. Health 19 (2021) 35. https://doi.org/10.3390/ijerph19010035.

[8]   M. Ferman, Winter storm could cost Texas more money than any disaster in state history, Tex. Trib. (2021).

[9]   L. Metzger, The Texas Freeze: Timeline of events, 2022. https://environmentamerica.org/texas/center/articles/the-texas-freeze-timeline-of-events.

[10] P. Svitek, Texas puts final estimate of winter storm death toll at 246, Tex. Trib. (2022). https://www.texastribune.org/2022/01/02/texas-winter-storm-final-death-toll-246/ (accessed July 24, 2022).

[11] H.R. Tiedmann, L.A. Spearing, S. Castellanos, K.K. Stephens, L. Sela, K.M. Faust, Tracking the post-disaster evolution of water infrastructure resilience: A study of the 2021 Texas winter storm, Sustain. Cities Soc. 91 (2023) 104417.

[12] D. Kyne, Winter storm URI 2021: a litmus test for extreme event resiliency, J. Extreme Events (2023) 2250004.

[13] S.E. Grineski, T.W. Collins, J. Chakraborty, E. Goodwin, J. Aun, K.D. Ramos, Social disparities in the duration of power and piped water outages in Texas after Winter Storm Uri, Am. J. Public Health 113 (2023) 30–34.

[14] B. Tomko, C.L. Nittrouer, X. Sanchez-Vila, A.H. Sawyer, Disparities in disruptions to public drinking water services in Texas communities during Winter Storm Uri 2021, PLOS Water 2 (2023) e0000137.

[15] Z. Shah, J.P. Carvallo, F.-C. Hsu, J. Taneja, The inequitable distribution of power interruptions during the 2021 Texas winter storm Uri, Environ. Res. Infrastruct. Sustain. 3 (2023) 025011.

[16] J. Xu, Y. Qiang, H. Cai, L. Zou, Power outage and environmental justice in Winter Storm Uri: an analytical workflow based on nighttime light remote sensing, Int. J. Digit. Earth 16 (2023) 2259–2278. https://doi.org/10.1080/17538947.2023.2224087.

[17] Y. Pi, X. Ye, N. Duffield, M.A. for H.A. Group, Rapid Damage Estimation of Texas Winter Storm Uri from Social Media Using Deep Neural Networks, Urban Sci. 6 (2022) 62.

[18] A. Hariharan, J.Y. Park, A flagged or spam? Social media driven public interactions for natural disaster response and recovery, in: Proc. 8th ACM Int. Conf. Syst. Energy-Effic. Build. Cities Transp., 2021: pp. 216–217.

[19] E. Terracciano, A.T. Han, Twitter communication during winter storm Uri in San Antonio, Texas-Implications for climate resiliency planning, Cities 139 (2023) 104407.

[20] S.E. Grineski, T.W. Collins, J. Chakraborty, Cascading disasters and mental health inequities: Winter Storm Uri, COVID-19 and post-traumatic stress in Texas, Soc. Sci. Med. 315 (2022) 115523.

[21] S. Castellanos, J. Potts, H. Tiedmann, S. Alverson, Y.R. Glazer, A. Robison, S. Russo, D. Harmon, B. Ken-Opurum, M. Weisz, A synthesis and review of exacerbated inequities from the February 2021 winter storm (Uri) in Texas and the risks moving forward, Prog. Energy 5 (2023) 012003.

[22] S. Gao, J. Rao, Y. Kang, Y. Liang, J. Kruse, Mapping county-level mobility pattern changes in the United States in response to COVID-19, SIGSpatial Spec. 12 (2020) 16–26.

[23] X. Hou, S. Gao, Q. Li, Y. Kang, N. Chen, K. Chen, J. Rao, J.S. Ellenberg, J.A. Patz, Intracounty modeling of COVID-19 infection with human mobility: Assessing spatial heterogeneity with business traffic, age, and race, Proc. Natl. Acad. Sci. 118 (2021). https://doi.org/10.1073/pnas.2020524118.

[24] Z. Zhou, Z. Xu, A. Liu, S. Zhou, L. Mu, X. Zhang, Mapping the accessibility of medical facilities of wuhan during the COVID-19 pandemic, ISPRS Int. J. Geo-Inf. 10 (2021) 318.

[25] B. Hong, B.J. Bonczak, A. Gupta, C.E. Kontokosta, Measuring inequality in community resilience to natural disasters using large-scale mobility data, Nat. Commun. 12 (2021) 1870. https://doi.org/10.1038/s41467-021-22160-w.

[26] C. Podesta, N. Coleman, A. Esmalian, F. Yuan, A. Mostafavi, Quantifying community resilience based on fluctuations in visits to points-of-interest derived from digital trace data, J. R. Soc. Interface 18 (2021) 20210158. https://doi.org/10.1098/rsif.2021.0158.

[27] A. Coston, N. Guha, D. Ouyang, L. Lu, A. Chouldechova, D.E. Ho, Leveraging Administrative Data for Bias Audits: Assessing Disparate Coverage with Mobility Data for COVID-19 Policy, in: Proc. 2021 ACM Conf. Fairness Account. Transpar., 2021: pp. 173–184.

[28] R.Z. Zhou, Y. Hu, J.N. Tirabassi, Y. Ma, Z. Xu, Deriving neighborhood-level diet and physical activity measurements from anonymized mobile phone location data for enhancing obesity estimation, Int. J. Health Geogr. 21 (2022) 1–18.

[29] K. Sun, Y. Hu, Y. Ma, R.Z. Zhou, Y. Zhu, Conflating point of interest (POI) data: A systematic review of matching methods, Comput. Environ. Urban Syst. 103 (2023) 101977.

[30] B. Zhang, Y. Dong, K. Kelobonye, R.Z. Zhou, Z. Xu, Delineating Walking Catchment of the Existing and Proposed Public Sports Facilities with Open-Source Data: A Case Study of Nanjing, Appl. Spat. Anal. Policy 16 (2023) 729–749.

[31] Z. Zhou, Z. Xu, Detecting the pedestrian shed and walking route environment of urban parks with open-source data: A case study in Nanjing, China, Int. J. Environ. Res. Public. Health 17 (2020) 4826.

[32] Pew Research Center, Demographics of Mobile Device Ownership and Adoption in the United States, Pew Res. Cent. Internet Sci. Tech (2021). https://www.pewresearch.org/internet/fact-sheet/mobile/ (accessed January 21, 2022).

[33] C.-C. Lee, M. Maron, A. Mostafavi, Community-scale big data reveals disparate impacts of the Texas winter storm of 2021 and its managed power outage, Humanit. Soc. Sci. Commun. 9 (2022) 335. https://doi.org/10.1057/s41599-022-01353-8.

[34] P. Chen, W. Zhai, X. Yang, Enhancing resilience and mobility services for vulnerable groups facing extreme weather: lessons learned from Snowstorm Uri in Harris County, Texas, Nat. Hazards (2023). https://doi.org/10.1007/s11069-023-06062-2.

[35] X. Huang, J. Lu, S. Gao, S. Wang, Z. Liu, H. Wei, Staying at home is a privilege: evidence from fine-grained mobile phone location data in the U.S. during the COVID-19 pandemic, Ann. Am. Assoc. Geogr. (2021) in press. https://doi.org/doi: 10.1080/24694452.2021.1904819.

[36] X. Huang, Y. Xu, R. Liu, S. Wang, S. Wang, M. Zhang, Y. Kang, Z. Zhang, S. Gao, B. Zhao, Z. Li, Exploring the spatial disparity of home-dwelling time patterns in the USA during the COVID-19 pandemic via Bayesian inference, Trans. GIS 26 (2022) 1939–1961. https://doi.org/10.1111/tgis.12918.

[37] Z. Wang, M.O. Román, Q. Sun, A.L. Molthan, L.A. Schultz, V.L. Kalb, Monitoring disaster-related power outages using NASA black marble nighttime light product, ISPRS Int Arch Photogramm Remote Sens Spat Inf Sci 2018 (2018) 1853–1856.

[38] Q. Zheng, Q. Weng, Y. Zhou, B. Dong, Impact of temporal compositing on nighttime light data and its applications, Remote Sens. Environ. 274 (2022) 113016.

[39] K. Watson, R. Cross, M. Jones, The Effects of the Winter Storm of 2021 in Harris County, Hobby Sch. Public Aff. Univ. Houst. (2021).

[40] C. Maxouris, Texas is still reeling from devastating winter storms and for some, recovery could take months, (2021). https://www.cnn.com/2021/02/22/us/texas-storm-recovery-monday/index.html.

[41] NOAA, Valentine's Week Winter Outbreak 2021: Snow, Ice, & Record Cold, 2021. https://www.weather.gov/hgx/2021ValentineStorm.

[42] R. Squire, What about bias in the SafeGraph dataset?, SafeGraph Blog (2019). https://www.safegraph.com/blog/what-about-bias-in-the-safegraph-dataset (accessed September 30, 2020).

[43] SafeGraph, Determining home location, (2020). https://docs.safegraph.com/docs/monthly-patterns#section-determining-home-location.

[44] M.O. Román, E.C. Stokes, R. Shrestha, Z. Wang, L. Schultz, E.A.S. Carlo, Q. Sun, J. Bell, A. Molthan, V. Kalb, Satellite-based assessment of electricity restoration efforts in Puerto Rico after Hurricane Maria, PloS One 14 (2019) e0218883.

[45] J. Xu, Y. Qiang, Spatial Assessment of Community Resilience from 2012 Hurricane Sandy Using Nighttime Light, Remote Sens. 13 (2021) 4128. https://doi.org/10.3390/rs13204128.

[46] NASA VIIRS Land Science Investigator-Led Processing System, VIIRS/NPP Gap-Filled Lunar BRDF-Adjusted Nighttime Lights Daily L3 Global 500m Linear Lat Lon Grid, (2019). https://doi.org/10.5067/VIIRS/VNP46A2.001.

[47] H. Cai, N.S.N. Lam, Y. Qiang, L. Zou, R.M. Correll, V. Mihunov, A synthesis of disaster resilience measurement methods and indices, Int. J. Disaster Risk Reduct. 31 (2018) 844–855. https://doi.org/10.1016/j.ijdrr.2018.07.015.

[48] Z. Wang, N.S.N. Lam, N. Obradovich, X. Ye, Are vulnerable communities digitally left behind in social responses to natural disasters? An evidence from Hurricane Sandy with Twitter data, Appl. Geogr. 108 (2019) 1–8. https://doi.org/10.1016/j.apgeog.2019.05.001.

[49] L. Zou, N.S.N. Lam, H. Cai, Y. Qiang, Mining Twitter Data for Improved Understanding of Disaster Resilience, Ann. Am. Assoc. Geogr. 108 (2018) 1422–1441. https://doi.org/10.1080/24694452.2017.1421897.

[50] NASA Earth Observatory, Extreme Winter Weather Causes U.S. Blackouts, 2021. https://earthobservatory.nasa.gov/images/147941/extreme-winter-weather-causes-us-blackouts.
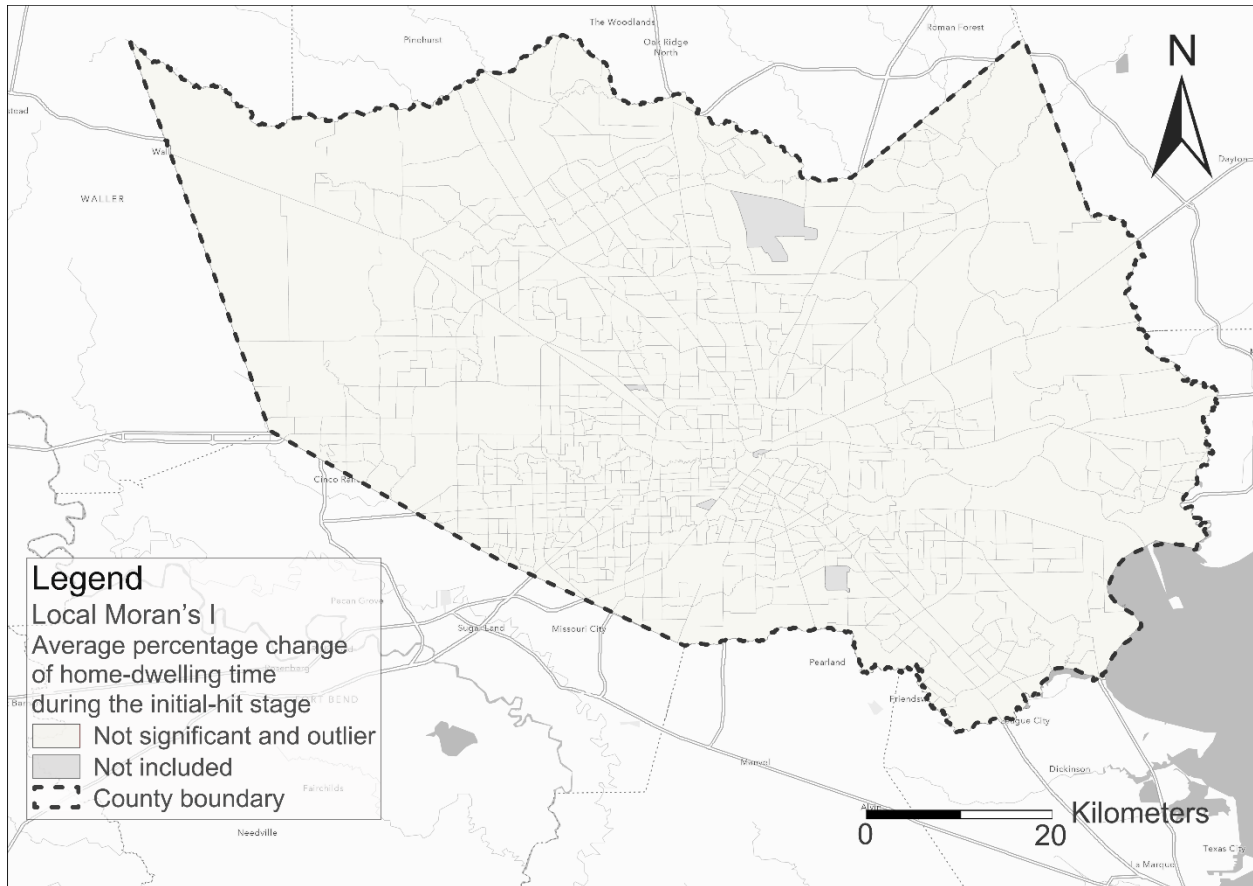
Supplementary Materials

Figure S1. Result of the local Moran's I analysis in the initial-hit stage based on the average percentage changes of home-dwelling time of census tracts.
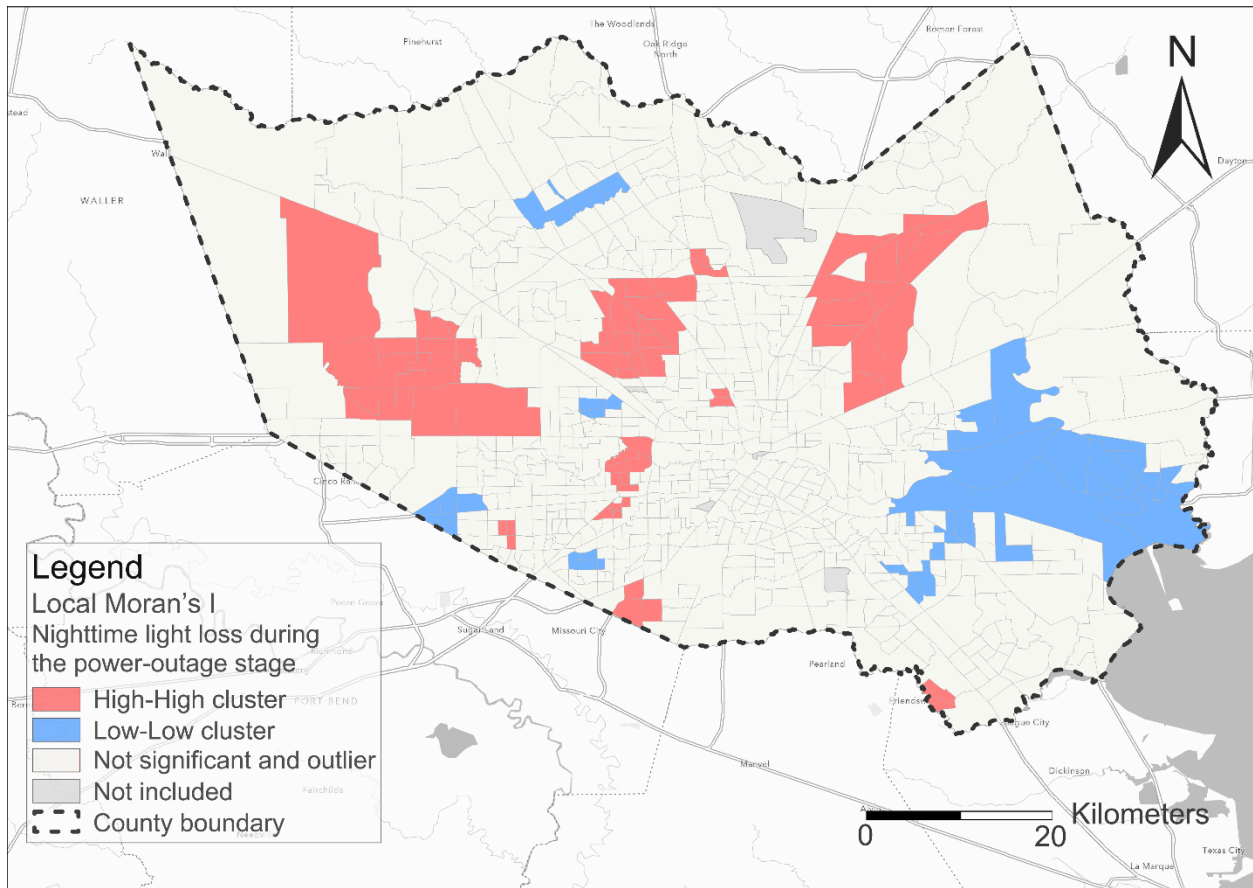
Figure S2. Result of the local Moran's I analysis in the power-outage stage based on the nighttime light loss of census tracts.
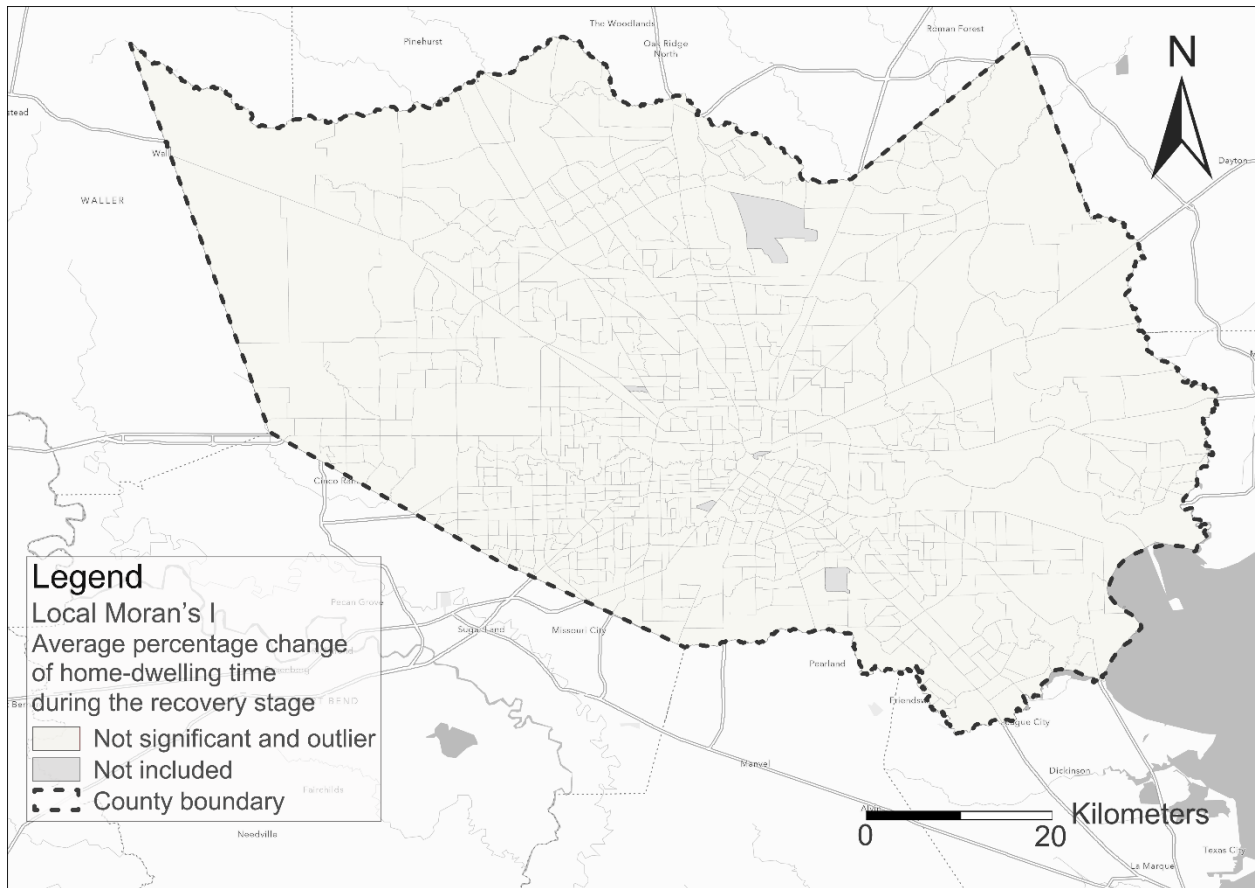
Figure S3. Result of the local Moran's I analysis in the recovery stage based on the average percentage changes of home-dwelling time of census tracts.